Ordered (3 × 4) High-Density Phase of Methylthiolate on Au(111)

Valentina De Renzi,*,† Rosa Di Felice,† Diego Marchetto,† Roberto Biagi,† Umberto del Pennino,† and Annabella Selloni‡

INFM Center for nanoStructures and bioSystem at Surfaces and Dipartimento di Fisica, Università di Modena e Reggio Emilia, Modena, Italy, and Department of Chemistry, Princeton University, Princeton, New Jersey 08544

Received: August 22, 2003; In Final Form: November 7, 2003

The formation of ordered phases of dimethyl-disulfide on the Au(111) surface has been investigated by means of low-energy electron diffraction (LEED), X-ray photoemission spectroscopy (XPS), and state-of-the-art density-functional theory (DFT) periodic supercell calculations. The LEED diffraction pattern, obtained after a production method that includes two-step dosing and prolonged postdeposition annealing, unambiguously corresponds to a novel phase that consists of (3 × 4) domains coexisting with the as-deposited ($\sqrt{3} \times \sqrt{3}$)R30° structure. XPS measurements indicate that the coverage of the new (3 × 4) superstructure is the same as that of the ($\sqrt{3} \times \sqrt{3}$)R30° phase. In both phases, the binding energy of the S $2p_{3/2}$ core-level peak is found to be 162.2 eV, corresponding to the formation of a thiolate layer. The DFT calculations allow us to identify a viable metastable (3 × 4) structure where the S headgroups of the CH_3S radicals select distinct adsorption sites; three quarters of them adsorb at bridge sites and one quarter at top sites. The relative energetics of the (3 × 4) and ($\sqrt{3} \times \sqrt{3}$)R30° configurations suggest that the two structures may coexist on the surface, in agreement with experimental data.

Introduction

Interfaces between organic molecules with sulfur-containing headgroups and noble metal surfaces represent a fruitful class of systems with potential relevance in new technological applications such as supramolecular assembly, wetting, and corrosion inhibition.[1] In particular, the capabilities of S headgroups to strongly bind to different metals is exploited in state-of-the-art processing to obtain functionalized surfaces[2] as well as templates for further organic-on-organic growth.[3,4] Despite the fact that alkanethiols $CH_3(CH_2)_{n-1}SH$ (Cn) on Au(111) are the best-studied systems among this class of self-assembled monolayers (SAMs), several questions are still open concerning their adsorption mechanism and the relevance of intermolecular interactions in driving their two-dimensional order. These are fundamental issues to be addressed for the achievement of full control on the structural and electronic properties of functionalized surfaces.[5]

One relevant point still to be elucidated is the role of the thiol chain length in determining the molecular self-assembly at full coverage. Long-chain alkanethiols have been shown to form a (3 × $2\sqrt{3}$) rectangular superlattice at full coverage[6−8] in a wide range of preparation conditions, including deposition from solution and from vapor, with and without postdeposition annealing. Whereas a sulfur-pairing model implying multiple S−Au interactions (e.g., S bonded both to Au and to other S atoms with different S−Au bonding strengths) was initially proposed for the (3 × $2\sqrt{3}$) unit cell in the cases of C10 and C8 on Au(111),[8−10] recent high-resolution X-ray spectroscopy (XPS) studies of similar-ordered decanethiol monolayers[11] reported a single S $2p_{3/2}$ core-level peak, suggesting a unique thiolate−gold interaction mechanism (e.g., S bonded only to Au atoms) for all the thiols in the unit cell. Therefore, it is still a matter of debate whether the (3 × $2\sqrt{3}$) phase is mainly due to layer−substrate coupling or should rather be ascribed to lateral chain−chain interactions possibly dictated by the existence of different S binding sites but with the same S−Au coupling.

Studies of shorter thiols where the chain−chain interactions are minimized were thus conceived to elucidate the above issue, and several ordered phases were reported. Focusing our attention on the shortest possible alkanethiol chains Cn with $n = 1$, we note in particular that Dishner et al.[12] observed by scanning tunneling microscopy (STM) the formation of both a (3 × $2\sqrt{3}$) structure and a ($2\sqrt{3} \times \sqrt{3}$)R30°-striped phase for methanethiol (C1, e.g., CH_3SH) SAMs on Au(111) at full and partial monolayer coverage, respectively. Recently, a He atom scattering (HAS) experiment found a new ordered phase obtained from dissociative adsorption of dimethyl-disulfide $(CH_3S)_2$ (DMDS) on Au(111) after a proper postdeposition annealing procedure, which has been interpreted as a (3 × $2\sqrt{3}$) rectangular reconstruction[13] with the same periodicity as that found for the longer chains. On the basis of this result, the authors suggested that the (3 × $2\sqrt{3}$) phase is energetically favored for all alkanethiols, independent of the chain length, and that its attainment is simply determined by a proper sample preparation. The existence of a complex phase diagram also in the cases where the alkylic chains are short and lateral coupling is expected to play a minor role in the monolayer aggregation may be interpreted as a signature of the fact that the complex reconstructions are prominently induced by S−Au interactions, which involve geometrically inequivalent but electronically similar binding sites[11] characterized by similar adsorption energies and thiolate coupling strengths.

From the theoretical point of view, density-functional theory (DFT)-based quantum mechanical computational techniques are

* Author to whom correspondence may be addressed. E-mail: vderenzi@unimore.it. Fax: +39-059-2055235.

† Università di Modena e Reggio Emilia and INFM.

‡ Princeton University.

10.1021/jp0365054 CCC: $27.50
Published on Web 12/06/2003

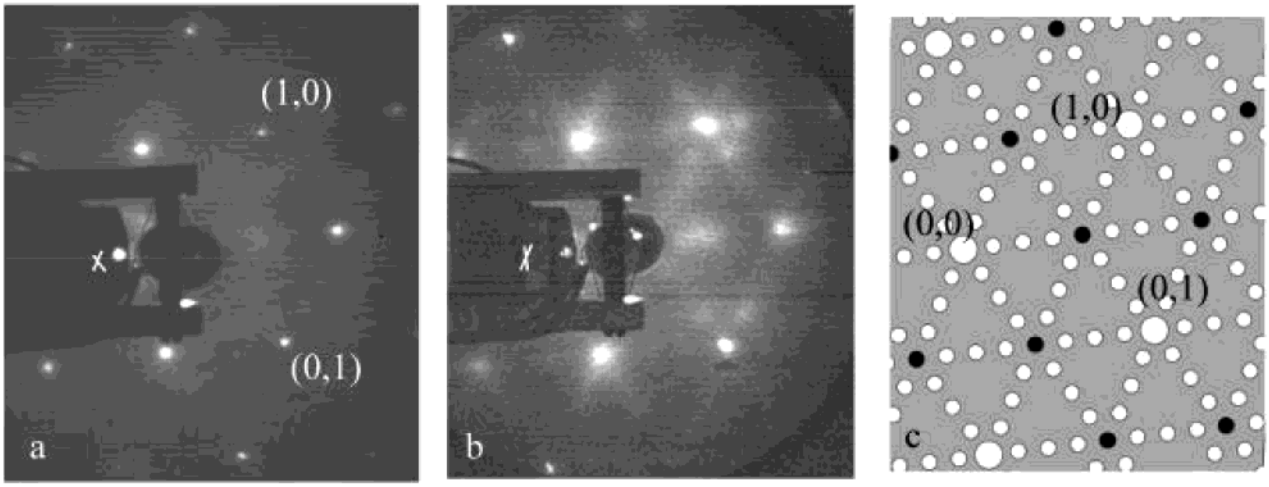

Figure 1. (a) LEED pattern of the ($\sqrt{3} \times \sqrt{3}$)R30° phase obtained by dosing 33 L DMDS at 200 K and subsequently annealing to 320 K for 2 min, taken at 100 K with electron beam energy $E_p = 60$ eV. The white cross indicates the specular peak position. (b) LEED pattern of the low-coverage phase, obtained after dosing 3 L DMDS at 100 K and subsequent annealing to 320 K for 2 min. XPS measurements on this surface indicated a fractional coverage of 0.66 relative to the ($\sqrt{3} \times \sqrt{3}$)R30° phase. (c) Scheme of the diffraction pattern of the ($4\sqrt{3} \times \sqrt{3}$)R30° superstructure. Large white circles represent integer-order spots and small black and white circles correspond to the ($\sqrt{3} \times \sqrt{3}$)R30° and ($4\sqrt{3} \times \sqrt{3}$)R30° spots, respectively.

suitable to characterize the surface superstructure induced by S−metal coupling but lack an accurate description of the interchain coupling; thus, they were mainly employed to describe short-chain thiols (in particular CH_3S, where the tailgroups are expected to play a minor role) on different surfaces.[14−16] On the contrary, classical molecular dynamics and mechanics have been the methods of choice to take into account the weak dispersion-like interactions between the molecular tailgroups of long-chain alkanethiols[17−19] but give a poor description of the S−metal interface bond. As a consequence, a direct energetical comparison of the two sets of alkanethiols (short-chain vs long-chain) is impossible on the basis of the available results and with the state-of-the-art computational settings. A combination of the quantum and the classical approaches may be the key to solve this long-standing controversy. An application of such a coupled quantum-mechanics/molecular-mechanics (QM/MM) scheme to the study of C10/Au(111) monolayers has only quite recently appeared,[20] shedding light onto several issues about the structure and the energetics of long-chain alkanethiol monolayers on metal surfaces. Whereas QM/MM computations are promising candidates for a solution of the long-standing controversies about the self-assembly of alkanethiol monolayers on metal surfaces, DFT calculations based on pure QM schemes currently remain a reliable and more affordable tool to investigate the interface features of short-chain thiolate layers.

Recent DFT calculations on the CH_3S/Au(111) system found the ($3 \times 2\sqrt{3}$) phase energetically indistinguishable from the ($\sqrt{3} \times \sqrt{3}$)R30° hexagonal lattice.[21] Despite the fact that this result is not able to explain the observation of the ($3 \times 2\sqrt{3}$) superstructure on the basis of a purely energetical point of view, it supports the existence of this phase as an equilibrium structure and confirms that its occurrence in the reality may be stimulated by the proper deposition technique. In a similar way, DFT calculations may be employed to analyze the geometry and the energetics of other surface reconstructions.

In this letter, we report the results of further experimental and theoretical investigations on the formation of ordered thiolate phases obtained by deposition of DMDS on the Au(111) surface. Following the recently proposed preparation procedure,[13] we observe by low-energy electron diffraction (LEED) the formation of a highly ordered (3×4) phase. In fact, the observed LEED pattern, which turns out to be fully compatible with the observations by Danişman et al.,[13] corresponds to the coexistence of both ($\sqrt{3} \times \sqrt{3}$)R30° and (3×4) phases rather than the proposed ($3 \times 2\sqrt{3}$) phase. On the basis of DFT calculations, we propose a viable model for the observed (3×4) reconstruction, whose molecular fractional coverage is the same as that of the ($\sqrt{3} \times \sqrt{3}$)R30° phase, in agreement with the indications of our XPS results. The calculated structure corresponds to a metastable phase, e.g., a local minimum of the potential-energy surface in the global phase space. The energetic relationship indicates that it is likely to coexist with the ($\sqrt{3} \times \sqrt{3}$)R30° order.[9,21]

Results and Discussion

The experiment is performed in an ultrahigh vacuum chamber (base pressure 1×10^{-10} mbar) where sputtering facilities, X-ray photoemission, and LEED equipments are available. The X-ray source (Mg K_α, photon energy $h\nu = 1253.6$ eV) is non-monochromatized, and the overall energy resolution is 2 eV. The sample is mounted on a cryogenic manipulator, and all measurements are performed at 100 K, if not otherwise stated. After the sample is cleaned by sputtering−annealing cycles, it is exposed to DMDS at 200 K. The DMDS exposure is performed by backfilling the chamber through a leak valve (typical dose pressure 4×10^{-7} mbar). Prior to every exposure, DMDS is purified by several freeze−pump−thaw cycles. Organic molecules are known to be significantly damaged by electron-beam irradiation. For this reason, we minimize the surface exposure to the LEED electron beam, maintaining the exposure time shorter than 1 min, with a beam-current density estimated to be about 50 nA/mm^2. In fact, under this current density, we observe in test measurements that the LEED pattern begins to deteriorate after a few minutes; on the basis of this evidence, we assume that for a short exposure the beam damage is a minor problem.

DMDS is expected to dissociate at room temperature (RT) on the Au(111) surface, forming a thiolate layer.[14,22,23] In our experiment, DMDS is dosed on the clean Au(111) surface at 200 K and subsequently annealed to 320 K.[13] Exposure to 33 L DMDS results in the formation of the well-known ($\sqrt{3} \times \sqrt{3}$)R30° phase, as shown in the LEED pattern

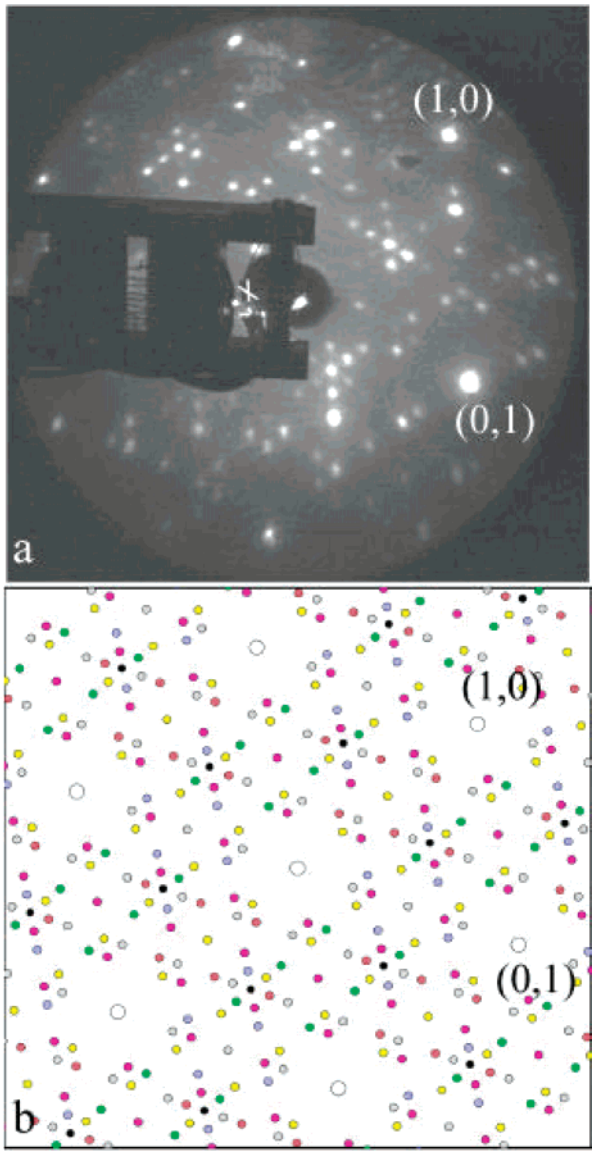

Figure 2. (a) LEED pattern of the coexisting (3 × 4) phase taken at 100 K with $E_p = 60$ eV. The specular beam position (white cross) and two integer order peaks are indicated. (b) Scheme of the diffraction patterns of the six equivalent domains of the (3 × 4) superstructure (small colored circles) and of the ($\sqrt{3} \times \sqrt{3}$)R30° superstructure (small black dots). White large circles correspond to the integer order peaks.

reported in Figure 1a. Interestingly, at lower coverage, the LEED pattern reveals, in addition to the spots of the ($\sqrt{3} \times \sqrt{3}$)R30° superstructure, the presence of weak satellites of the integer-order peaks and some streaky features connecting both integer- and fractional-order spots (see Figure 1b). This pattern can be tentatively assigned to the formation of small islands with different ($n\sqrt{3} \times \sqrt{3}$)R30°-striped phases, the position of the satellite spots fitting in particular with $n = 4$. In Figure 1c, the calculated LEED pattern for a ($4\sqrt{3} \times \sqrt{3}$)R30° superstructure is shown for comparison. This finding is in substantial agreement with the STM observation of a striped phase at low coverage,[12] which is determined by missing rows of molecules in the ($\sqrt{3} \times \sqrt{3}$)R30° lattice.

Following the procedure by Danişman and co-workers,[13] the well-ordered ($\sqrt{3} \times \sqrt{3}$)R30° phase, obtained by exposing a freshly prepared Au(111) surface to 33 L DMDS and annealing to 320 K, is then further exposed to 300 L DMDS, while ramping the temperature between 200−273 K. The sample is subsequently annealed at RT overnight, eventually obtaining the LEED pattern shown in Figure 2a. This pattern is due to the coexistence of the ($\sqrt{3} \times \sqrt{3}$)R30° phase with a new (3 × 4) phase, as shown schematically in Figure 2b.[24] For the sake of clarity, we refer in the following to this complex structure as the coexisting (3 × 4) phase. It is important here to notice that the observed LEED pattern does not fit with that of a (3 × $2\sqrt{3}$) superstructure. On the other hand, it compares quite well with the recently published HAS contour plot.[13] Because of the relatively low resolution of the HAS apparatus, the data by Danişman and co-workers[13] cannot indeed discriminate between the two structures.

The average fractional coverage of the coexisting (3 × 4) phase, as determined by XPS measurements, is the same as that of the ($\sqrt{3} \times \sqrt{3}$)R30° structure. Moreover, the shape and energy position of the S 2p core-level peak (not shown) is the same for both phases and corresponds to a thiolate layer (S $2p_{3/2}$ at 162.2 eV binding energy). A small component at 164.1 eV is observed in both spectra, which may be attributed to a small fraction of molecules not directly bound to the metal surface.[25] No atomic sulfur contribution is detected at the lower binding energy side of the S 2p spectra.

The presence of local (3 × 4) ordered structures on the CH_3S/Au(111) system was already observed by STM at low temperature by Kondoh and Nozoye,[26] who suggested that a phase transition from the (3 × 4) to the ($\sqrt{3} \times \sqrt{3}$)R30° phase would occur upon passing from low temperature (110 K) to RT. To check this indication, we investigate the temperature dependence of the LEED pattern of both the ($\sqrt{3} \times \sqrt{3}$)R30° and the coexisting (3 × 4) phases between 100−330 K. In the case of the ($\sqrt{3} \times \sqrt{3}$)R30° phase, no structural change can be observed by LEED in this temperature range. On the other hand, the coexisting (3 × 4) phase displays a strong temperature dependence: (i) A reversible disappearance of the (3 × 4) spots around 300 K may tentatively be interpreted as the fingerprint of a first-order (3 × 4)−($\sqrt{3} \times \sqrt{3}$)R30° phase transition, in partial agreement with the STM findings and (ii) upon annealing to 330 K the coexisting (3 × 4) phase irreversibly changes into the ($\sqrt{3} \times \sqrt{3}$)R30° phase, in agreement with previous experimental reports.[13] A thorough temperature-dependent characterization of the coexisting (3 × 4) structure is currently the object of further investigations.

To complement the experimental data and support the existence of a (3 × 4) reconstruction for the thiolated Au(111) surface, we perform ab initio plane-wave pseudopotential DFT-PW91 periodic slab calculations.[27] The positions of all the atoms in the supercell are relaxed in the potential energy determined by the full quantum mechanical electronic structure until the forces vanish within a precision of 0.03 eV/Å. The electron−ion interaction in the DFT total energy functional is described by non-norm-conserving pseudopotentials[28] for the species C, H, and Au, whereas S is represented by a norm-conserving pseudopotential.[29] The electron wave functions are expanded in a plane-wave basis set up to a kinetic energy cutoff of 20 Ryd. The surface is simulated with a supercell having a 3 × 4 periodicity, containing 4 Au layers with 12 atoms each, 4 CH_3S molecules adsorbed at one surface in the slab, and a vacuum thickness of 12 Å to avoid spurious interactions between neighboring replicas (see Figure 3). Four special **k** points are included in Brillouin Zone (BZ) sums. The computational details were previously validated by tests on similar systems.[21,23]

Our calculations allow us to identify a metastable (3 × 4) structure, shown in Figure 3, where the S headgroups of the CH_3S radicals select distinct adsorption sites; three quarters of them adsorb at bridge sites B1 and B2 (including bridging

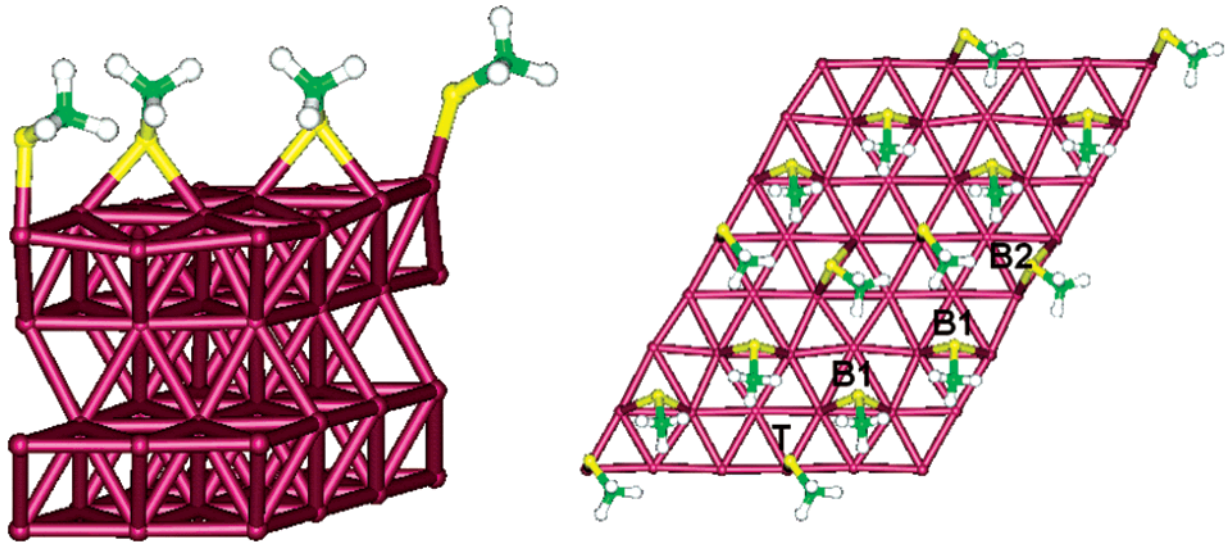

Figure 3. Left: three-dimensional view of the equilibrium structure. Right: top view of the equilibrium structure where it is clear that three quarters of the thiols adsorb at bridge sites (half at B1 along lattice vector $\mathbf{a}_1$, one quarter at B2 along lattice vector $\mathbf{a}_2$) and one quarter of the thiols adsorb at top sites (T), forming stripes along the major diagonal of the unit cell. Purple, yellow, green, and white spheres represent Au, S, C, and H atoms, respectively.

directions along both the independent basis vectors of the hexagonal lattice) and one quarter at top sites T of the (111) *fcc* lattice. The thiols are distributed in stripes that are approximately parallel to the major diagonal. Along such stripes, there are two inequivalent S−S distances equal to 4.25 and 4.83 Å for the bridge−top and the bridge−bridge pairs, respectively. The C−S bond distance is 1.87 Å for all the thiols in the unit cell, whereas the inclination of such bonds with respect to the surface normal varies between 42 and 58° for the molecules with the S headgroups anchored at B sites, and is 64° for those at T sites. The average S−Au distance is 2.5 Å (2.4 Å at the T site), typical of thiolate−gold interfaces independent of the detailed reconstruction and even of the molecular adsorbate; for instance, the S−Au distance is the same when cysteine is the adsorbed molecule.[23] The topmost Au layer is strongly corrugated, by about 0.3 Å.

Our finding of two different binding sites cannot be directly compared to the recent experimental indication in favor of adsorption of methylthiolate at the T site only because the latter experiment addresses a different geometry, namely the $(\sqrt{3} \times \sqrt{3})$R30° phase.[30] We also remark that the presence of two different adsorption sites does not contradict our observation of a single S 2p core-level component. In fact, while both B and T sites support a thiolate−gold interaction of similar strength, the energy resolution of our apparatus (~2 eV) is too low to allow us to clearly distinguish between such sites. However, a more detailed investigation of this question, including high resolution measurements as well as calculations of core-level binding-energy differences, would be certainly worthwhile.

To support the viability of the optimized (3 × 4) geometry, we compare its total energy with that of the $(\sqrt{3} \times \sqrt{3})$R30° structure; for the latter, we choose the lowest-energy configuration[21] with all the S headgroups adsorbed at bridge sites and thus equally spaced by 5.1 Å, a S−Au distance of 2.5 Å, the S−C bonds forming an angle of 56° with respect to the surface normal, and a topmost Au corrugation of 0.3 Å. We find that the computed (3 × 4) geometry is slightly energetically unfavored relative to the $(\sqrt{3} \times \sqrt{3})$R30° phase by about 1 kcal/mol,[31] in agreement with the experimental observation of the coexistence between the two phases. This energy difference is in fact quite small and could be considered inside the uncertainty of the method. We note that both the occurrence of two different bridge sites (see B1 and B2 in Figure 3) and the energetic balance between the (3 × 4) extended-cell superstructure and the basic hexagonal $(\sqrt{3} \times \sqrt{3})$R30° geometry are in line with similar results of the recent QM/MM computations for the $(3 \times 2\sqrt{3})$ monolayers of decanethiols on Au(111).[20] Although the structures and the molecules are different in the two cases, the similarities suggest common effects due to the S−Au interactions. Whereas it is not possible at the adopted level of theory to discriminate between the relative importance of molecule−substrate and molecule−molecule coupling in the determination of complex reconstructions for C1/Au(111), the present calculations support the suggestion that a complex energy landscape and phase diagram of thiolated surfaces is characteristic also of short-chain alkanethiols.

Conclusions

In conclusion, we unambiguously determine a novel coexisting (3 × 4) long-range ordered phase of the CH_3S/Au(111) system, obtained after a recently proposed dosing−annealing procedure[13] suitable to produce ordered thiolate monolayers on Au(111) from vapor-phase DMDS. This phase is characterized by the coexistence of the well-known $(\sqrt{3} \times \sqrt{3})$R30° with a new (3 × 4) superstructure. Preliminary indications of a structural phase transition around 300 K are inferred by the analysis of the LEED temperature dependence and suggest that the subtle energetic balance between the (3 × 4) and the $(\sqrt{3} \times \sqrt{3})$R30° phases is influenced by temperature. LEED measurements also indicate that at low coverage a striped phase is formed, characterized by small islands of $(n\sqrt{3} \times \sqrt{3})$R30° order, in agreement with STM observations.[12] A viable theoretical model for the (3 × 4) superstructure is proposed, which is found to be metastable and with a formation energy higher by only 1 kcal/mol with respect to the $(\sqrt{3} \times \sqrt{3})$ hexagonal phase, thus justifying their coexistence. Our results therefore confirm, in agreement with HAS measurements,[13] that different ordered phases are likely to occur at full coverage also for the smallest thiolate precursor. In the case of the CH_3S/Au(111), the observation of a long-range ordered (3 × 4) phase different from the $(3 \times 2(\sqrt{3})$ superstructure suggests that the molecular chain

length plays a significant role in the determination of the thiolate geometrical details. Interestingly, a local (3×4) phase has been also observed with STM for ethanethiol layers on Au(111),[32] thus suggesting that this superstructure could be a common feature of short-chain alkanethiolate overlayers on the Au(111) surface. To this regard, we wish to point out that the complex thermal behavior of the (3×4) phase, as well as the need for a proper preparation procedure involving successive steps of exposure and annealing, are still open issues that deserve future investigation.

Finally, we would like to remark that the availability of different ordered superstructures of thiolate interfaces could be possibly exploited in soft-on-soft epitaxy to tailor the template geometrical properties.

Acknowledgment. M. Borsari and co-workers are acknowledged for experimental support. The authors are grateful to L. Casalis and G. Scoles for useful discussions and for sharing unpublished details of their data. Computing time at CINECA is provided by INFM through the Parallel Computing Committee. Funding is provided by INFM through PRA SINPROT, by MIUR (Italy) through FIRB NOMADE, and by the EC through Contract IST-2000-28024 "SAMBA".

References and Notes

(1) Ulman, A. *Chem. Rev.* **1996**, *96*, 1533.
(2) Otsubo, T.; Aso, Y.; Takimiya, K. *J. Mater. Chem.* **2002**, *12*, 2565.
(3) Gerstenberg, M. C.; Schreiber, F.; Leung, T. Y. B.; Bracco, G.; Forrest, S. R.; Scoles, G. *Phys. Rev. B* **2000**, *61*, 7678.
(4) Staub, R.; Toerker, M.; Fritz, T.; Schmitz-Hübsch, T.; Sellam, F.; Leo, K. *Surf. Sci.* **2000**, 445, 368.
(5) Schreiber, F. *Prog. Surf. Sci.* **2000**, *65*, 151
(6) Camillone, N.; Chidsey, C. E. D.; Liu, G.-y.; Scoles, G. *J. Chem. Phys.* **1993**, *93*, 98.
(7) Poirier, C. E.; Tarlov, M. J. *Langmuir* **1994**, *10*, 2853.
(8) Fenter, P.; Eberhardt, A.; Eisenberger, P. *Science* **1994**, *266*, 1216.
(9) Fenter, P.; Schreiber, F.; Berman, L.; Scoles, G.; Eisenberger, P.; Bedzyk, M. J. *Surf. Sci.* **1998**, *413*, 213.
(10) Kluth, G. J.; Carraro, C.; Maboudian, R. *Phys. Rev. B* **1999**, *59*, R10449.
(11) Yang, Y. W.; Fan, L. J. *Langmuir* **2002**, *18*, 1157.
(12) Dishner, M. H.; Hemminger, J. C.; Feher, J. C. *Langmuir* **1997**, *13*, 2318.
(13) Danişman, F. M.; Casalis, L.; Bracco, G.; Scoles, G. *J. Phys. Chem. B* **2002**, *106*, 11771.
(14) Grönbeck, H.; Curioni, A.; Andreoni, W. *J. Am. Chem. Soc.* **2000**, *122*, 2839.
(15) Hayashi, T.; Morikawa, Y.; Nozoye, H. *J. Chem. Phys.* **2001**, *114*, 7615−7621.
(16) Molina, L.; Hammer, B. *Chem. Phys. Lett.* **2002**, *360*, 264.
(17) Sprik, M.; Delamarche, E.; Michel, B.; Röthlisberger, U.; Klein, M. L.; Wolf, H.; Ringsdorf, H. *Langmuir* **1994**, *10*, 4116.
(18) Gerdy, J. J.; Goodard, W. A., III. *J. Am. Chem. Soc.* **1996**, *118*, 3233.
(19) Bhatia, R.; Garrison, B. J. *Langmuir* **1997**, *13*, 4038.
(20) Fischer, D.; Curioni, A.; Andreoni, W. *Langmuir* **2003**, *19*, 3567.
(21) Vargas, M. C.; Giannozzi, P.; Selloni, A.; Scoles, G. *J. Chem. Phys. B* **2001**, *105*, 9509.
(22) Nuzzo, R. G.; Zegarski, B. R.; Dubois, L. H. *J. Am. Chem. Soc.* **1987**, *109*, 9, 733.
(23) Di Felice, R.; Selloni, A.; Molinari, E. *J. Phys. Chem. B* **2003**, *107*, 1151.
(24) Although a few spots of the (3×4) superstructure are missing in the LEED image shown in Figure 2a, they are clearly visible in the LEED pattern taken at different beam energies and/or geometrical conditions, unequivocally confirming the superstructure identification.
(25) Heister, K.; Zharnikov, M.; Grunze, M.; Johansson, L. S. O.; Ulman, A. *Langmuir* **2001**, *17*, 8.
(26) Kondoh, H.; Nozoye, H. *J. Phys. Chem. B* **1999**, *103*, 2585.
(27) We used the code PWSCF by Baroni, S.; Dal Corso, A.; de Gironcoli, S.; Giannozzi, P., available at http://www.pwscf.org.
(28) Vanderbilt, D. *Phys. Rev. B* **1990**, *41*, 7892.
(29) Troullier, N.; Martins, J. L. *Phys. Rev. B* **1992**, *46*, 1754.
(30) Kondoh, H.; Iwasaki, M.; Shimada, T.; Amemiya, K.; Yokoyama, T.; Ohta, T.; Shimomura, M.; Kono, S. *Phys. Rev. Lett.* **2003**, *90*, 066102.
(31) To obtain this relative formation energy, the total energy of the 3×4 structure optimized with 4 **k** points was calculated with a uniform mesh of 8 special **k** points in the irreducible BZ and compared to the total energy of the $\sqrt{3} \times \sqrt{3}$ structure computed with a uniform mesh of 24 special **k** points in the irreducible BZ to achieve a comparable sampling.
(32) Kawasaki, M.; Nagayama, H. *Chem. Lett.* **2001**, *30*, 942.